Macromolecules

Article

Cite This: Macromolecules 2019, 52, 2939−2948

pubs.acs.org/Macromolecules

pH-Dependent Morphology and Photoresponse of Azopyridine-Terminated Poly(*N*-isopropylacrylamide) Nanoparticles in Water

Hao Ren,[†] Xing-Ping Qiu,[‡] Yan Shi,[§] Peng Yang,[†] and Françoise M. Winnik*[,∥,⊥]

[†]Key Laboratory of Applied Surface and Colloid Chemistry, Ministry of Education, School of Chemistry and Chemical Engineering, Shaanxi Normal University, Xi'an 710119, China

[‡]Department of Chemistry, University of Montreal, CP 6128 Succursale Centre Ville, Montreal, Quebec H3C 3J7, Canada

[§]School of Materials Science and Engineering, Beijing University of Chemical Technology, Beijing 100029, P. R. China

[∥]Laboratory of Polymer Chemistry, Department of Chemistry, University of Helsinki, PB 55, Helsinki FI00140 Finland

[⊥]International Center for Materials Nanoarchitectonics, National Institute for Materials Science, 1-1 Namiki, Tsukuba 305-0044, Japan

Supporting Information

ABSTRACT: A series of azopyridine-terminated poly(*N*-isopropylacrylamide)s (PNIPAM) (C12-PN-AzPy) (~5000 < M_w < 20 000 g mol^{-1}, polydispersity index 1.25 or less) were prepared by reversible addition−fragmentation chain-transfer polymerization of NIPAM in the presence of a chain-transfer agent that contains an AzPy group and an *n*-dodecyl chain. In cold water, the polymers form nanoparticles (5.9 nm < R_h < 10.9 nm) that were characterized by light scattering (LS), ^{1}H NMR diffusion experiments, and high-resolution transmission electron microscopy. We monitored the pH-dependent photoisomerization of C12-PN-AzPy nanoparticles by steady-state and time-resolved UV−vis absorption spectroscopy. Azopyridine is known to undergo a very fast cis-to-trans thermal relaxation when the azopyridine nitrogen is quaternized or bound to a hydrogen bond donor. The cis-to-trans thermal relaxation of the AzPy chromophore in an acidic nanoparticle suspension is very fast with a half-life τ = 2.3 ms at pH 3.0. It slows down slightly for nanoparticles in neutral water (τ = 0.96 s, pH 7.0), and it is very slow for AzPy-PNIPAM particles in alkaline medium (τ > 3600 s, pH 10). The pH-dependent dynamics of the cis-to-trans dark relaxation, supported by Fourier transform infrared spectroscopy, ^{1}H NMR spectroscopy, and LS analysis, suggest that in acidic medium, the nanoparticles consist of a core of assembled C12 chains surrounded by a shell of hydrated PNIPAM chains with the AzPy$^+$ end groups preferentially located near the particle/water interface. In neutral medium, the shell surrounding the core contains AzPy groups H-bonded to the amide hydrogen of the PNIPAM chain repeat units. At pH 10.0, the amide hydrogen binds preferentially to the hydroxide anions. The AzPy groups reside preferentially in the vicinity of the C12 core of the nanoparticles. The morphology of the nanoparticles results from the competition between the segregation of the hydrophobic and hydrophilic components and weak attractive interactions, such as H-bonds between the AzPy groups and the amide hydrogen of the PNIPAM repeat units.

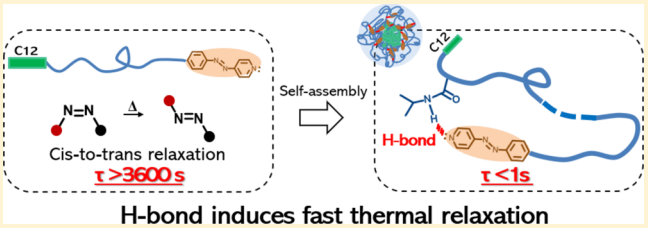

1. INTRODUCTION

Among the various stimuli for responsive polymer-based devices, light possesses several advantages: it is directional, tunable in terms of energy, and it can be turned on and off rapidly.[1−3] Azobenzene, which undergoes reversible trans-to-cis photoisomerization, is commonly used for such applications. The trans-to-cis isomerization requires UV light irradiation. The cis-to-trans back-conversion occurs upon irradiation with visible light and also by thermal relaxation in the dark.[4,5] The thermal cis-to-trans relaxation of azobenzene is very slow. It takes several hours for completion. Disubstituted azobenzenes, such as 4-*N*,*N*-dimethylamino-4′-nitro-azobenzene, undergo thermal cis-to-trans isomerization much faster, with relaxation times on the order 10−100 μs.[6,7] The fast response results from the "push−pull" electronic distribution imposed by the electron donor and the electron-withdrawing substituents linked to the 4 and 4′ positions, respectively. This speed is critical for applications that require real-time information without the use of a second photostimulation to regenerate the trans form, an important thrust in current material science.

Replacement of one phenyl ring of azobenzene with a pyridinium ring has a similar effect on the π-electron distribution of azo chromophores, as exemplified by azopyridinium methyl iodide for which the cis-to-trans thermal relaxation time is on the order of 10−100 μs.[6] The pyridine ring nitrogen is a powerful H-bond acceptor,[8] a property employed extensively in the construction of supermolecular

Received: January 27, 2019
Revised: March 17, 2019
Published: April 1, 2019

DOI: 10.1021/acs.macromol.9b00193
Macromolecules 2019, 52, 2939−2948

Scheme 1. Synthetic Pathways to α-Azobenzene-, α-Azopyridine-, and α-Ethyl-azopyridinium-ω-n-dodecyl-PNIPAMs

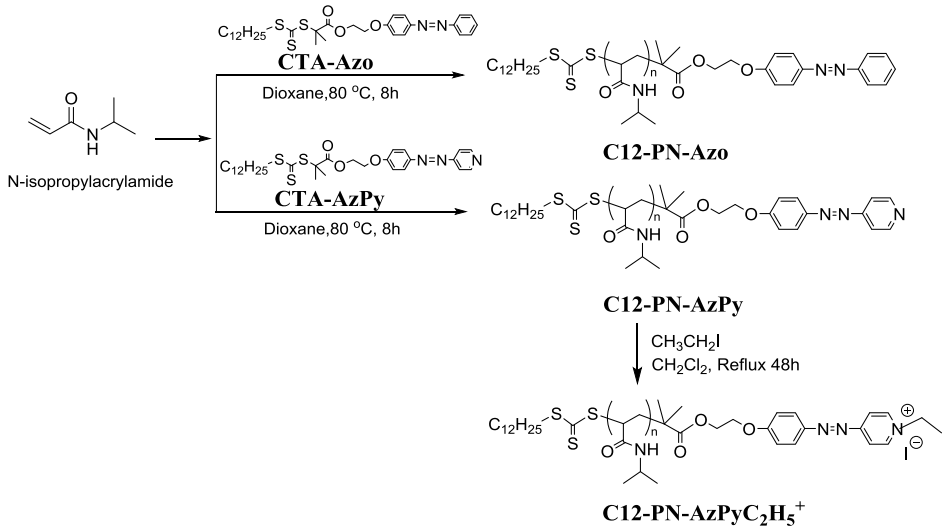

assemblies, such as liquid crystals,[9−11] metal−organic frameworks,[12,13] fibers,[14] films,[15,16] and gels.[17−19] It turns out that binding of the AzPy nitrogen to common H-bond donors, such as phenols, accelerates the cis-to-trans thermal relaxation rate of neutral AzPy because of the redistribution of the AzPy π-electron imposed by the H-bond formation. This effect was exploited recently by Gelebart et al. who succeeded in generating continuous, macroscopic mechanical waves by continuous irradiation of films containing AzPy H-bonded to benzoic acid moieties.[16]

In spite of such spectacular achievements, the design of simple, easily controllable, and fast-relaxing azo systems remains challenging, particularly in the case of water-borne polymeric materials.[20,21] Amphiphilic copolymers containing AzPy have been reported and evaluated in solutions, microparticles, and nanoparticles in suspensions or as hydrogels.[19,22] For instance, Zhang et al. reported that AzPy-containing poly(*N*-isopropylacrylamide) (PNIPAM) block copolymers in water form giant vesicles, which undergo photocontrolled swelling and shrinking.[17−19] Supramolecular hydrogels formed by coassembly of phenylalanine-based amphiphiles and AzPy moieties were shown to undergo macroscopic gel−sol transition in response to light and also through changes in temperature, or pH.[23] The dynamics of the thermal cis−trans relaxation were not assessed in these studies.

We report here the preparation of amphiphilic PNIPAM bearing an AzPy moiety on one chain end and an *n*-dodecyl group on the other end, as simple models to evaluate the dynamics of neutral and charged AzPy in aqueous environments. A series of polymers (C12-PN-AzPy) of well-defined molar mass were synthesized by reversible addition−fragmentation chain-transfer (RAFT) polymerization using a chain-transfer agent bearing AzPy and *n*-dodecyl groups (Scheme 1). Light-scattering (LS) measurements, ^{1}H NMR spectroscopy diffusion, and fluorescence probe studies indicate that the polymers self-assemble in neutral water to form colloidally stable nanoparticles. The photophysical properties of the colloidal dispersions were monitored as a function of the dispersion pH. Transient absorption spectroscopy measurements indicated that the cis-to-trans thermal relaxation of AzPy is sluggish in alkaline dispersions of C12-PN-AzPy but extremely fast in acidic and, unexpectedly, in neutral dispersions of the polymer. The fast dynamics of the cis-to-trans dark relaxation exhibited by neutral C12-PN-AzPy suggest that the AzPy end groups form H-bonds with the amide hydrogens of the PNIPAM repeat units in neutral conditions. This hypothesis was confirmed by several control measurements. It led us to conclude that C12-PN-AzPy chains do not form typical core−shell flower micelles but adopt a more complex morphology that varies depending on the solution pH. This result is of interest in the context of polymer self-assembly and also from the practical view point as an entry to fast responsive light-driven systems.

2. EXPERIMENTAL SECTION

2.1. Materials. *N*-Isopropylacrylamide was purchased from Sigma-Aldrich and recrystallized using hexane. The initiator 4,4′-azobis(4-cyanovaleric acid) (ACPA, 97%) was purchased from Sigma-Aldrich and recrystallized using methanol. The RAFT agent *S*′-1-dodecyl-*S*′-(α,α′-dimethyl-α″-acetic acid) trithiocarbonate (CTA-1) was synthesized as described earlier.[24] 2-(4-(Pyridin-4-yldiazenyl)phenoxy)-ethan-1-ol (HO-C_2-AzPy) and 2-(4-(phenyldiazenyl)phenoxy)ethan-1-ol (HO-C_2-Azo) were synthesized by known procedures.[10,25] All other reagents were obtained from Sigma-Aldrich and were used as received.

2.2. Synthesis of RAFT Agents CTA-AzPy and CTA-Azo (See Scheme S1). *2.2.1. 2-(4-(Pyridin-4-yldiazenyl)phenoxy)ethyl 2-(((dodecylthio)carbonothioyl)thio)-2-methylpropanoate (CTA-AzPy).* A solution of dicyclohexylcarbodiimide (DCC, 0.66 g, 3.2 mmol) in CH_2Cl_2 (10 mL) was added dropwise to a solution of 2-(dodecylthiocarbonothioylthio)-2-methylpropionic acid (CTA-1, 1.0 g, 2.8 mmol) and HO-C_2-AzPy (0.68 g, 2.8 mmol) in CH_2Cl_2 (20 mL) kept in an ice/water bath. After 12 h at rt, the solid was removed by filtration, and the solvent was stripped off by evaporation. The solid residue was purified by chromatography over a silica column eluted with hexane/ethyl acetate (4/1, v/v) as the eluent. A yellow solid (1.2 g, yield 72%) was obtained. ^{1}H NMR ($CDCl_3$): δ 8.79 (d, *J* = 8.0 Hz, 2H), δ 7.96 (d, *J* = 8.0 Hz, 2H), δ 7.68 (d, *J* = 8.0 Hz, 2H), δ 7.03 (d, *J* = 8.0 Hz, 2H), δ 4.51 (t, *J* = 4.0 Hz, 2H), δ 4.27 (t, *J* = 4.0 Hz, 2H), δ 3.14 (t, *J* = 8.0 Hz, 2H), δ 1.71 (s, 6H), δ 1.58 (m, 2H), δ 1.22 (br, 20H), δ 0.88 (t, *J* = 6.5 Hz, 3 H) (Figure S1). The ^{13}C NMR and the two-dimensional heteronuclear multiple quantum correlation (2D-HMQC) spectra of CTA-AzPy are shown in Figures S2 and S3. The mass spectrum is given in Figure S4.

2.2.2. 2-(4-(Phenyldiazenyl)phenoxy)ethyl 2-(((dodecylthio)-carbonothioyl)thio)-2-methylpropanoate (CTA-Azo). A solution of DCC (0.66 g, 3.2 mmol) in CH_2Cl_2 (10 mL) was added dropwise to a solution of CTA-1 (1.0 g, 2.8 mmol) and 2-(4-(phenyldiazenyl)-

DOI: 10.1021/acs.macromol.9b00193
Macromolecules 2019, 52, 2939−2948

phenoxy)ethan-1-ol (HO-C_2-Azo, 0.67 g, 2.8 mmol) in CH_2Cl_2 (20 mL) kept in an ice/water bath. After 12 hours at room temperature (rt), the solid was removed by filtration. The filtrate was evaporated to dryness. The solid residue was purified by chromatography over a silica column eluted with hexane/ethyl acetate (4/1, v/v) as the eluent. An orange solid (1.1 g, yield 65%) was obtained. ^{1}H NMR ($CDCl_3$): δ 7.93 (m, 4H), δ 7.52 (m, 3H), δ 7.03 (d, J = 12.0 Hz, 3H), δ 4.53 (t, J = 4.8 Hz, 2H), δ 4.27 (t, J = 4.8 Hz, 2H), δ 3.16 (t, J = 8.0 Hz, 2H), δ 1.73 (s, 6H), δ 1.60 (m, 2H), δ 1.24 (br, 20H), δ 0.90 (t, J = 6.8 Hz, 3 H) (Figure S1).

2.3. General Procedure for the Synthesis of End-Functionalized PNIPAMs. The polymers were prepared by RAFT polymerization of NIPAM in the presence of either CTA-AzPy or CTA-Azo. The following procedure leading to C12-PN-AzPy 12K is typical. In a 50 mL flask, NIPAM (1.13 g, 10 mmol), CTA-AzPy (0.059 g, 0.1 mmol), and ACPA (0.0056 g, 0.02 mmol) were dissolved in 1,4 dioxane (10 mL). 1,3,5-Trioxane (0.02 g) was added to the solution as an internal reference for ^{1}H NMR measurements monitoring the progress of the polymerization. The solution was degassed with nitrogen for 30 min at rt. The flask was placed in a preheated oil bath set at 80 °C and kept at this temperature for 6 h. The polymerization mixture was cooled to rt, and the polymer was purified by three consecutive precipitations into hexane. The sample was further purified by dialysis against water for 3 days and isolated by freeze-drying. See Figures S5 and S6 for the ^{1}H NMR spectra of C12-PN-AzPy and C12-PN-Azo.

2.4. Quaternization of the Azopyridium End Group of AzPy-Terminated PNIPAM. Iodoethane (0.5 mL, 6.25 mmol) was added to a solution of C12-PN-AzPy 12K (0.45 g) in CH_2Cl_2 (10 mL). The reaction mixture was refluxed at 40 °C for 5 days, while monitoring the degree of advancement of the reaction by ^{1}H NMR spectroscopy. After completion of the reaction, the solvent was removed by evaporation. The polymer was dissolved in methanol, dialyzed against water for 3 days, and isolated by freeze-drying (0.56 g) as an orange powder. See Figures S7 for the ^{1}H NMR spectra of the region part of C12-PN-AzPy 12K and C12-PN-AzPy$C_2H_5^+$ 12K.

2.5. Characterization. *2.5.1. Instrumentation.* ^{1}H NMR spectra were recorded on a Bruker AMX-400 (400 MHz) spectrometer. NMR diffusion experiments were performed with a Bruker AVANCE III (500 MHz) at 10 °C. Molecular weights and molecular weight distributions were determined with an Agilent 1100 gel permeation chromatography (GPC) system fitted with a TSK-gel R-M column [particle size 13 μm, exclusion limit 1 × 10^7 Da for polystyrene in dimethylformamide (DMF)] and a TSKgel R-3000 column (particle size 7 μm, exclusion limit 1 × 10^5 Da for polystyrene in DMF) (Tosoh Biosep); DMF containing 0.4 wt % LiBr was used as the eluent and the flow rate was set at 0.5 mL/min; the column temperature was set at 40 °C. Mass spectra were acquired on an Agilent 6224 Accurate-Mass time-of-flight liquid chromatography–mass spectrometry. Fourier transform infrared (FTIR) spectra were recorded on a Nicolet 8700 FTIR spectrometer. Critical aggregation concentration (CAC) values determined by a fluorescence probe were conducted using a Varian fluorimeter (Agilent Technologies).

2.5.2. Determination of the Polymer Molar Mass from UV–Vis Absorption Data. The molecular weight was determined according to eq 1

$$M_n = \frac{w}{c_{CTA}} \tag{1}$$

where w is the weight of the polymer in the solution (in grams) and c_{CTA} is the amount of RAFT agent residues (end groups of the polymer) in solution (in mol), determined experimentally by application of Beer's law. Gaussian functions were used to separate the overlapping absorbances of the trithiocarbonate, azopyridine, or azobenzene chromophores (fitting from 270 to 450 nm). The molar extinction coefficients of the trithiocarbonate, the azopyridine and the azobenzene chromophores in methanol are ε_{310nm} = 20 400 L mol^{-1} cm^{-1}, ε_{355nm} = 24 700 L mol^{-1} cm^{-1}, and ε_{351nm} = 18 700 L mol^{-1} cm^{-1}, respectively.

2.5.3. Solution Preparation. For LS experiments, polymer solutions were prepared by dissolution in water of a suitable weighed amount of polymer. Solutions were refrigerated (~5 °C) for at least 24 h before analysis to ensure complete polymer dissolution. For the pH-dependent tests, the solution pH was adjusted by dropwise addition of 0.1 M NaOH or 0.1 M HCl to neutral polymer solutions. Solutions were refrigerated at least 24 h before testing.

2.5.4. Critical Aggregation Concentration (CAC) of Polymeric Micelles. The CAC of the modified PNIPAM samples was determined with Nile red (NR) as the fluorescence probe. Solutions for analysis were prepared as follows. A drop of a concentrated NR solution in ethanol was placed in a vial and the solvent was evaporated with a flow of nitrogen. Aqueous polymer solutions ranging in concentration from 0.001 to 5.0 mg/mL were prepared by dilution with water of a polymer stock solution (5.0 mg/mL). The solutions were placed in the vials containing NR and refrigerated for at least 24 h before measurement. The excitation wavelength was set at 520 nm, and both the excitation and emission slits were set at 5 nm. The CAC values were determined by two methods for accuracy, one is the inflection point of plots of the fluorescence maximum wavelength versus the logarithm of the polymer concentration and another one is the onset of the increase of the fluorescence intensity at 630 nm versus the logarithm of the polymer concentration.

2.5.5. Light-Scattering Measurements. Dynamic light-scattering (DLS) and static light-scattering (SLS) studies were carried out with a light-scattering (LS) system equipped with a CGS-3 goniometer (ALV GmbH) fitted with an ALV/LSE-5003 multiple correlator (ALV GmbH) and a C25P temperature controller (Thermo Haake). The light source was a He–Ne laser (632 nm). Polymer solutions in water were refrigerated overnight and filtered through a 0.2 μm Millex Millipore PVDF filter prior to analysis.

In SLS experiments, the scattering intensity was measured at several angles from 30 to 150° against a toluene standard. The time-averaged excess scattered intensity at angle θ, also known as the Rayleigh ratio $R_{vv}(q)$, was related to the weight-averaged molar mass M_w, the Z-averaged root-mean-square radius R_g, the second virial coefficient A_2, and the scattering vector (q), where $K = 4\pi^2 n^2 (dn/dc)^2/(N_A\lambda_0^4)$ and $q = (4\pi n/\lambda_0)\sin(\theta/2)$, with N_A, n, (dn/dc), and λ_0 being Avogadro's constant, the refractive index of the solvent, the specific refractive index increment of the solution, and the wavelength of light in vacuum, respectively. The dn/dc value of PNIPAM in water was assumed to be independent of temperature and equal to 0.167 mL/g.[26] The partial Zimm plot and the aggregation number N_{agg} for aggregates were obtained from eqs 2 and 3

$$\frac{Kc}{R_{vv}(q)} = \frac{1}{M_w}\left(1 + \frac{1}{3}R_g^2 q^2\right) + 2A_2 c \tag{2}$$

$$N_{agg} = \frac{M_{w.micelle}}{M_{w.polymer}} \tag{3}$$

For DLS, the $g^2(q,t)$ autocorrelation functions from DLS analysis for each angle were analyzed by the CONTIN algorithm to determine the relaxation time, Γ. The Γ values at each angle were plotted against the square of the scattering wave vector (q), and the diffusion coefficient (D) was calculated from $D = (\Gamma/q^2)_{q\to 0}$. The hydrodynamic radius (R_h) is given by the Stokes–Einstein equation, $R_h = k_B T/(6\pi\eta D)$, where k_B is the Boltzmann constant, T is the absolute temperature, and η is the solvent viscosity.

2.5.6. NMR Diffusion Measurements. Diffusion experiments were carried out with a Bruker AVANCE 500 NMR spectrometer operating at the amplitude g of the pulsed field gradients stepped up linearly from 15 to 300 G cm^{-1} in 16 steps using a stimulated echo sequence with gradient pulses of a length of δ = 2 ms. The total diffusion time was Δ = 100 ms.

Polymer diffusion coefficients (D) were obtained by fitting to a Gaussian decay, see eq 4

$$\frac{S}{S_0} = \exp\left[-\gamma^2\delta^2 g^2 D\left(\Delta - \frac{\delta}{3}\right)\right] \tag{4}$$

DOI: 10.1021/acs.macromol.9b00193
Macromolecules 2019, 52, 2939–2948

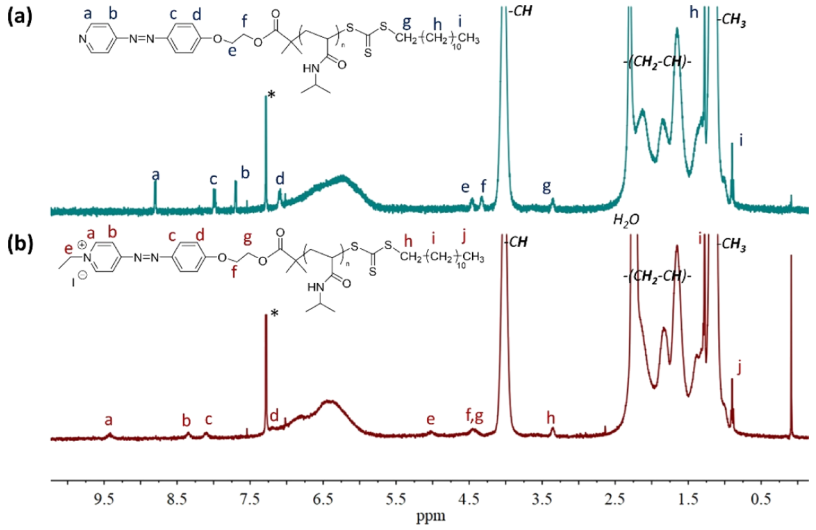

Figure 1. ^{1}H NMR spectra and spectral assignments of (a), C12-PN-AzPy 12K, and (b) C12-PN-AzPyC$_2$H$_5^+$ 12K. (The residual solvent CDCl$_3$ singlet is marked with *.)

where S and S_0 are the integral intensities with and without gradient, which were calculated from the resonance of the $-CH_3$ protons (δ: 0.621−1.153 ppm); γ is the magnetogyric ratio (4.258×10^3 Hz/G in this case), and g is the amplitude of the magnetic field gradient (17.8125 G cm^{-1}/step in this case). The operating temperature was 10 °C. All polymer solutions (1.0 mg/mL in D_2O) were refrigerated for at least 24 h prior to measurements.

2.5.7. Irradiation Experiments. Photoisomerization tests were carried out with a Prizmatix light-emitting diode (LED) light source emitting at a wavelength of 365 nm (50 mW). The photoisomerization measurements were conducted at 15 °C for all samples. A polymer solution (2 mL) was placed in a 10 mm cuvette and irradiated. Absorbance spectra of the sample were measured as a function of irradiation time.

2.5.8. Thermal Relaxation Kinetics. The relaxation of azopyridine group under neutral conditions was determined with a UV−vis spectrometer (LAMBDA 750, PerkinElmer) at rt. A 365 nm LED−UV lamp holder was placed above the solution kept in the dark prior to irradiation. The changes with time of the absorbance intensity at 355 nm were recorded upon UV irradiation until the initial intensity value was recovered. The time interval between each measurement was set at 0.2 s. The relaxation kinetics were fitted with the stretched exponential function defined in eqs 5 and 6[16]

$$A(t) = A_\infty - (A_\infty - A_0)e^{-(kt)^\beta} \quad (5)$$

$$\tau = \sqrt[\beta]{\ln(2)}/k \quad (6)$$

where k is the fitting constant; β the stretched exponential parameter; τ the half-life of *cis*-azopyridine; and A_0, $A(t)$, and A_∞ are the absorbances at 355 nm before UV irradiation, after UV irradiation at time t, and in the photostationary state, respectively.

2.5.9. Transient Absorption Measurements. The relaxation rate of the *N*-ethyl *cis*-azopyridinium moiety in C12-PN-AzPyC$_2$H$_5^+$ (12K) was measured at rt with a laser flash photolysis system (LP 920, Edinburgh Instruments). The laser wavelength was 355 nm. The pulse time was 10 ns with an energy of 10 mJ/pulse. The detection wavelength was 365 nm. The data were fit with the exponential function defined in eq 7

$$\Delta OD(t) = \Delta OD_0 \exp[-t/\tau] \quad (7)$$

where ΔOD_0 is the initial optical density, τ is the relaxation time, and ΔOD is the time-dependent optical density.

2.5.10. Transmission Electron Microscopy Measurements. Transmission electron microscopy (TEM) images were recorded with a Tecnai G2 F20 at 200 kV (FEI, USA), equipped with a 4k charge-coupled device camera. An aqueous solution of C12-PN-AzPy 20K (0.5 mg mL^{-1}) was kept at 5 °C for at least 24 h. One drop of the cold solution was deposited on a carbon-coated copper grid placed on a filter paper. The prepared TEM grid was dried at rt under vacuum before measurement.

3. RESULTS AND DISCUSSION

3.1. Synthesis and Characterization of End-Modified PNIPAM Derivatives. The polymers were prepared by RAFT polymerization of NIPAM in dioxane using the chain-transfer agents CTA-AzPy or CTA-Azo, the latter CTA leading to azobenzene-modified PNIPAM used in control experiments described below (Scheme 1). The structure of the two CTAs was confirmed by their ^{1}H NMR, ^{13}C NMR, and 2D-HMQC NMR spectra, shown in Figures S1−S3 and their purity was ascertained by high-resolution mass spectrometry (Figure S4). By changing the NIPAM to CTA-AzPy molar ratio in the polymerization mixture, we obtained five samples of C12-PN-AzPy ranging in molar mass from 5000 to 20 000 g/mol. The successful incorporation of the hydrophobic C12 group on one end of the polymer chains and of the AzPy group on the other was confirmed by the ^{1}H NMR and UV−vis absorption spectra of the polymers. Figure 1a presents the ^{1}H NMR spectrum of C12-PN-AzPy-12K in CDCl$_3$. It features a triplet at 0.88 ppm, ascribed to the resonance of the terminal methyl protons of the dodecyl chain and signals in the aromatic spectral region ascribed to the azopyridine protons: signals a and b are attributed to the protons of the pyridine ring while the signals c and d correspond to the protons of the aromatic ring connected to the polymer by an ether bond. The presence of the trithiocarbonate function on the ω-end of the polymer is confirmed by the polymer UV−vis absorption spectrum, which features a band centered at 310 nm, attributed to the trithiocarbonate, in addition to a band at 355 nm ascribed to the AzPy chromophore linked at the α-end (Figure S9b). The azopyridine group was quaternized by reaction of C12-PN-AzPy with ethyl iodide. The structure of the resulting polymer, C12-PN-AzPyC$_2$H$_5^+$, was confirmed by its ^{1}H NMR spectrum, see Figure 1b. The aromatic signals of the spectrum of C12-PN-AzPy underwent a downfield shift upon quaternization of the pyridine ring, as expected in view of the strong electron-withdrawing effect of the pyridinium ring.[27] Signals character-

DOI: 10.1021/acs.macromol.9b00193
Macromolecules 2019, 52, 2939−2948

istic of the azopyridine protons cannot be detected in the spectrum of the quaternized compound, a good indication that the quaternization went to near completion.

The molar mass (M_n) of the polymers was determined by GPC with multiangle LS detection. The polydispersity index of the polymers also obtained from the GPC data ranges between 1.03 and 1.25 and the degree of polymerization (DP) varies from 32 to 162. The molar mass values determined from the ratio of the area of the PNIPAM methine (−C***H***) resonance in their ^{1}H NMR spectrum to that of the signal attributed to the resonance of H_a on the azopyridine group, using $M_{n\ NMR} = (2 \times I_{-CH}/I_{H_a}) \times 113.2 + M_{CTA\text{-}AzPy}$, as well as the UV−vis absorption-derived M_n values (see Figure S9 in the case of C12-PN-AzPy, 12K) agree well with the GPC-derived values (Table 1).

Table 1. Molar Mass and Polydispersity Index of the Polymers Prepared

	M_n (g/mol)				
sample name	UV	GPC	NMR	DP[a]	M_w/M_n[b]
C12-PN-AzPy 5K	5500	5800	4200	32	1.25
C12-PN-AzPy 7K	7700	7800	7900	60	1.03
C12-PN-AzPy 12K	12 400	12 900	10 700	110	1.09
C12-PN-AzPy$C_2H_2^+$ 12K		12 900	10 700	110	1.09
C12-PN-AzPy 20K	19 500	19 700	19 000	162	1.03
C12-PN-Azo 12K	12 600	13 600	12 500	115	1.23

[a]DP from the NMR spectra of polymer solutions in $CDCl_3$. [b]Determined by GPC.

3.2. Solution Properties of the Polymers in Water (10 °C). LS is a powerful technique to characterize the size and structure of self-assembled amphiphilic PNIPAMs.[28,29] DLS gives information on the hydrodynamic radius (R_h) and SLS provides the radius of gyration (R_g) as well as the average molecular weight ($M_{w.micelle}$) and aggregation number (N_{agg}) of the micelles.[30,31] DLS and SLS analyses of C12-PN-AzPy solutions at 10 °C revealed the presence of nanoparticles. Their size and aggregation characteristics are listed in Table 2.

The R_h and R_g values of the nanoparticles increase with increasing polymer molar mass, in agreement with related previous studies.[29,32] The aggregation number (N_{agg}) of the nanoparticles, obtained from LS and NMR diffusion experiments (see Figures S10 and S11), decreases with increasing molar mass of the polymers. The structure parameter, $\rho = R_g/R_h$, which reflects the mass distribution of the scattering object, is useful to assess the morphology of self-assembled nanoparticles.[26,31] The R_g/R_h values of all C12-PN-AzPy nanoparticles in water (10 °C) range from 1.37 to 1.48, a range of values characteristic of random coils and of core/shell particles with a solvated shell. TEM images of dried C12-PN-AzPy suspensions provide further support to the size of the micelles and the formation of core/shell assemblies (Figure 2c,d). The

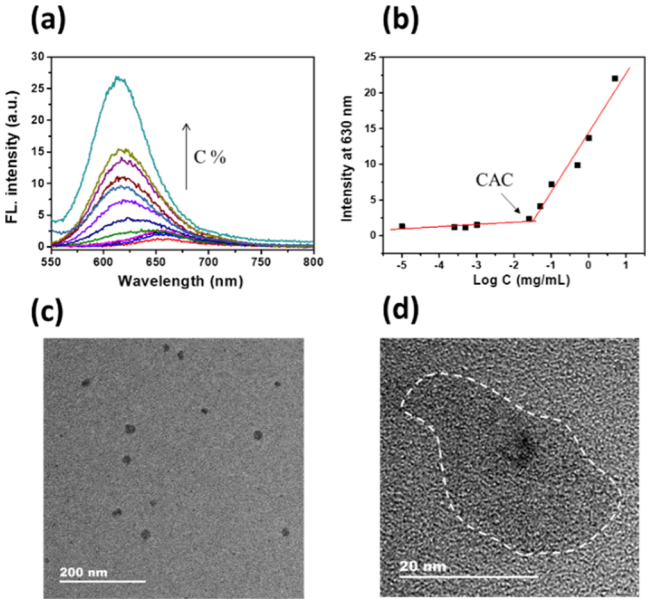

Figure 2. (a) Fluorescence spectra of NR in C12-PN-AzPy 12K aqueous solutions of increasing polymer concentration (λ_{ex} = 530 nm; slits: 5 nm; temperature, 10 °C). (b). Plot of the NR fluorescence emission intensity at 630 nm as a function of C12-PN-AzPy 12K concentration. (c) TEM images and (d) high-resolution electron TEM images of C12-PN-AzPy 20K 0.5 mg/mL.

higher contrast of the particle core, visualized by high-resolution TEM, suggests that the core contains closely packed hydrophobic end groups (Figure 2d). The critical aggregation concentration (CAC) of the C12-PN-AzPy samples was evaluated by fluorescence spectroscopy using NR. This probe was selected as its absorption window (λ_{max} = 520 nm) does not overlap with the absorption spectra of the AzPy and trithiocarbonate chromophores (see Figure S9).[32,33] The emission of NR is affected by the polarity of the probe environment: as the polarity of the environment decreases, the excitation and emission spectra of NR shift to shorter wavelengths and the emission intensity increases[34,35] as shown in Figure 2a in the case of C12-PN-AzPy 12K. Figures 2b and S12 present the experimental data used to determine the CAC of this polymer in water from the changes with polymer concentration of the NR emission intensity and emission wavelength, respectively. The CAC values of the

Table 2. Characteristics of the C12-PN-AzPy Nanoparticles in Water (10 °C,[d] 10 mg/mL)

sample name	CAC (g/L)[a]	N_{agg}[b]	R_g (nm)[b]	R_h (nm)[b]	R_h (nm)[c]	R_g/R_h
C12-PN-AzPy 5K	0.002−0.008	19[e]	9.2[e]	6.3[e]	5.9	1.46
C12-PN-AzPy 7K	0.003−0.006	18[e]	10.2[e]	7.4[e]	7.9	1.37
Cl2-PN-AzPy 12K	0.025−0.032	15	15.6	10.5	8.0	1.48
C12-PN-AzPy$C_5H_5^+$ 12K	0.037−0.043	13	20.0	14.0	8.6	1.43
C12-PN-AzPy 20K	0.039−0.035	10	14.6	10.5	10.9	1.39
C12-PN-Azo 12K	0.008−0.010	19	13.5	8.2		1.64

[a]Determined from the inflection points of plots of the maximum NR emission wavelength and of the fluorescence emission intensity at 630 nm versus polymer concentration. [b]Determined by DLS. [c]Determined by NMR diffusion experiments. [d]This temperature is below the cloud point of all solutions, as described in a forthcoming article. [e]Some large aggregates in suspension were removed by filtration prior to measurements.

DOI: 10.1021/acs.macromol.9b00193
Macromolecules 2019, 52, 2939−2948

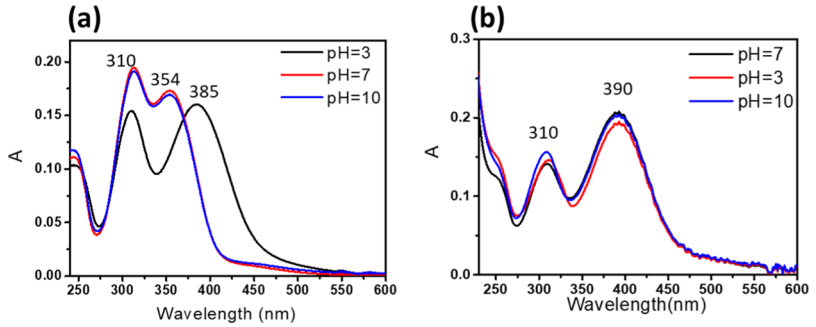

Figure 3. UV−vis spectra of (a) C12-PN-AzPy 7K (0.1 mg/mL) and (b) C12-PN-AzPyC$_2$H$_5^+$ (0.2 mg/mL) under different pH values (temperature 15 °C).

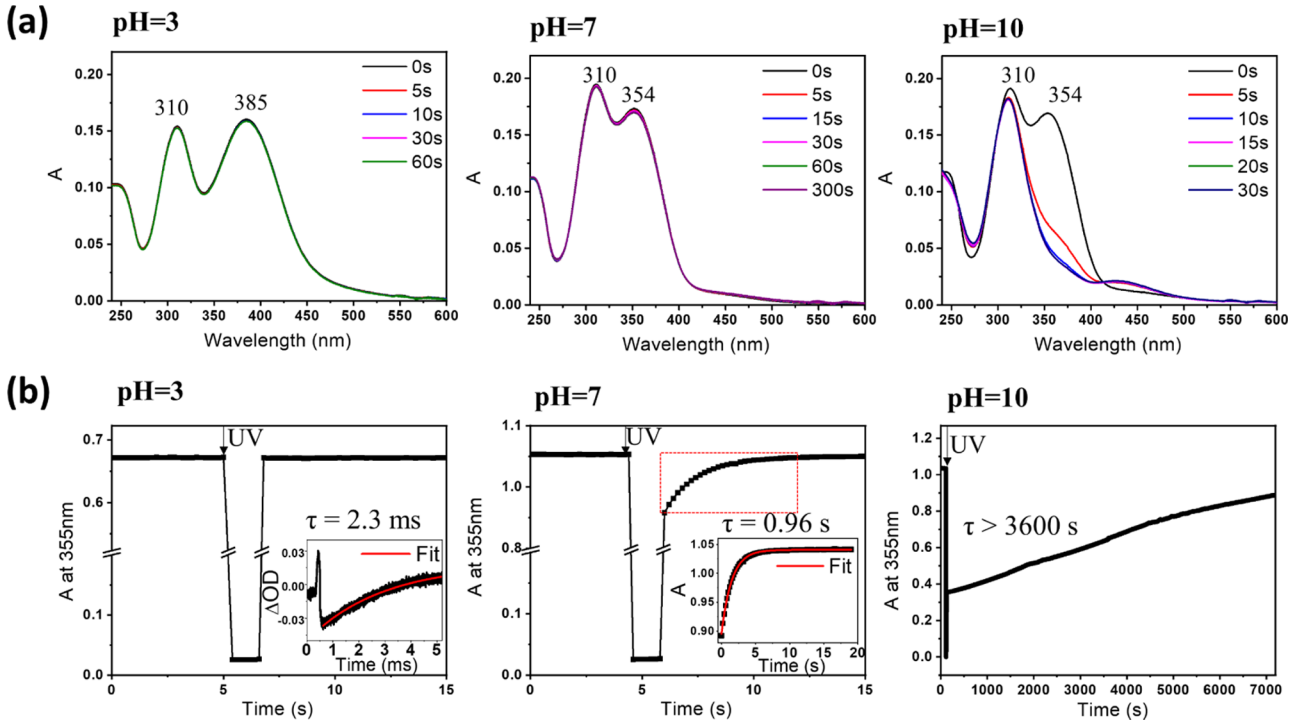

Figure 4. (a) UV−vis absorption spectra of C12-PN-AzPy 7K aqueous solutions (0.1 mg/mL, pH = 3.0, 7.0, 10.0) upon irradiation at 365 nm (LED−UV lamp, 50 mW/cm^2, temperature: 15 °C) and (b) transient absorption monitored at 355 nm of the same samples irradiated for 2 s at 365 nm.

C12-PN-AzPy samples increase by a factor of 10 with increasing polymer molar mass, within the 5−20 kg/mol molar mass range sampled here (Table 2), in agreement with related studies.[29]

Table 2 also presents the size of nanoparticles obtained for C12-PN-AzPyC$_2$H$_5^+$ 12K. Both R_g and R_h are significantly larger than the corresponding neutral polymer nanoparticles, but their ratio is not affected, implying that the overall core−shell morphology of the particles is preserved. The N_{agg} of the C12-PN-AzPyC$_2$H$_5^+$ 12K micelles decreases slightly, compared to C12-PN-AzPy 12K.

3.3. pH-Dependent Photophysical Properties of C12-PN-AzPy Nanoparticles in Water (15 °C). *3.3.1. UV−Vis Absorption Spectrum of Aqueous C12-PN-AzPy 7K Solutions (0.1 mg/mL, pH 3, 7, 10.).* As the pK_a of AzPy is ∼4.53,[36] spectra recorded for solutions of pH 7 and 10 correspond to the chromophore in its neutral form, whereas the spectrum measured at pH 3 is characteristic of the azopyridinium-protonated form (Figure 3a).[37,38] The UV spectra of solutions of C12-PN-AzPy 7K of pH 7 and 10 present a band at 354 nm, characteristic of the $\pi-\pi^*$ transition of the *trans*-azopyridine group. This band undergoes a red shift from 354 to 385 nm upon protonation of the pyridine group at pH 3. The red shift results from the strong push−pull electronic redistribution from the oxygen atom of the alkoxy substituent to the positively charged nitrogen atom of the azopyridium group. Similarly, the UV−vis spectra of aqueous C12-PN-AzPyC$_2$H$_5^+$ solutions, presented in Figure 3b, have a band at 390 nm, independently of the solution pH, as expected because the *N*-ethyl-pyridinium group is not pH responsive.[6,39] The UV−vis spectra of all samples (Figure 3a) have an additional band centered at 310 nm attributed to the $\pi-\pi^*$ transition of the thiocarbonyl group linked to the ω-chain end.[38] It will not be included in the following discussions as the thiocarbonyl chromophore is inert at all pH values under the irradiation conditions used here. We confirmed by ^{1}H NMR spectroscopy that the ester that links the azopyridine group to the polymer main chain is not hydrolyzed when the polymers are kept at

DOI: 10.1021/acs.macromol.9b00193
Macromolecules 2019, 52, 2939−2948

Scheme 2. Schematic Representation of C12-PN-AzPy Nanoparticles Dispersed in Water of pH 3, 7, and 10 Based on Data from LS, FTIR, and ^{1}H NMR Measurements and on the Kinetics of the cis-to-trans Thermal Relaxation of Azopyridine

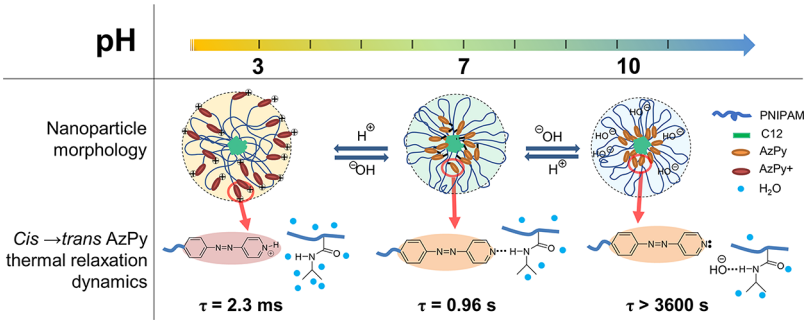

pH 3 or 10 for up to 5 days at rt and ∼1 day when heated to 70 °C (Figures S13 and S14.).

3.3.2. Photoisomerization of C12-PN-AzPy 7K. Aqueous solutions of C12-PN-AzPy 7K in water (pH 3, 7, and 10) were irradiated at 365 nm for 60 s and monitored by UV−vis absorption spectroscopy (Figure 4a). The UV−vis absorption spectrum of the polymer solution at pH 3 does not change throughout the irradiation time. Transient absorption measurements indicate that the relaxation rate is extremely fast (τ = 2.3 ms, Figure 4 pH = 3, inset) so that the absorption spectrum of the cis-isomer cannot be detected by steady-state absorption measurements. Similarly, transient absorption data recorded with the quaternized sample C12-PN-AzPyC$_2$H$_5^+$ yielded a half-lifetime value of 2.1 ms for the cis-isomer (Figure S15). These data are in full agreement with the known characteristics of the cis-to-trans isomerization of quaternized azopyridine.[6] A schematic representation of a C12-PN-AzPyH$^+$ micelle is drawn in Scheme 2 (left). The micelle contains a hydrophobic core formed by closely packed *n*-dodecyl chains surrounded by a shell of hydrated PNIPAM chains. The AzPyH$^+$ moieties are expected to be located near the water/micelle interface in view of their amphiphilicity.

The UV−vis absorption spectrum of the C12-PN-AzPy 7K solution at pH 7, where the azopyridine is in its neutral form, does not change, even after extended irradiation times (up to 300 s). Transient measurements indicate that the thermal cis-to-trans relaxation half-life is ∼0.96 s (Figure 4b, pH = 7, inset) (stretched exponential function, eq 5, Experimental Section). On the basis of previous studies of neutral AzPy, the fast back-relaxation is an indication that the AzPy nitrogen forms H-bonds with available H-donors. Within the C12-PN-AzPy nanoparticle environment, the abundant amide groups of the PNIPAM chains can readily form H-bonds with the azopyridine nitrogen. To test this hypothesis, we measured the ^{1}H NMR spectrum of a physical mixture of PNIPAM homopolymer and CTA-AzPy (5 mol %) in $CDCl_3$ prepared by evaporation of a solution of PNIPAM and CTA-AzPy in tetrahydrofuran and subsequent dilution in $CDCl_3$.[40] The signals of the aromatic protons of the azopyridine groups exhibit downshifts in the presence of PNIPAM, from 8.77 to 8.84 ppm for proton a and from 7.68 to 7.93 ppm for proton b (Figure 5b). The observed shifts are indicative of the delocalization of the π electrons of the azopyridine group. Moreover, the aromatic signals are broader in the spectrum of the mixed solution, compared to the original CTA spectrum (Figure 5a). The broadening of the NMR signals indicates a decrease of the CTA mobility, which is consistent with the coupling of the azopyridine to the PNIPAM chain via hydrogen bonding.[41]

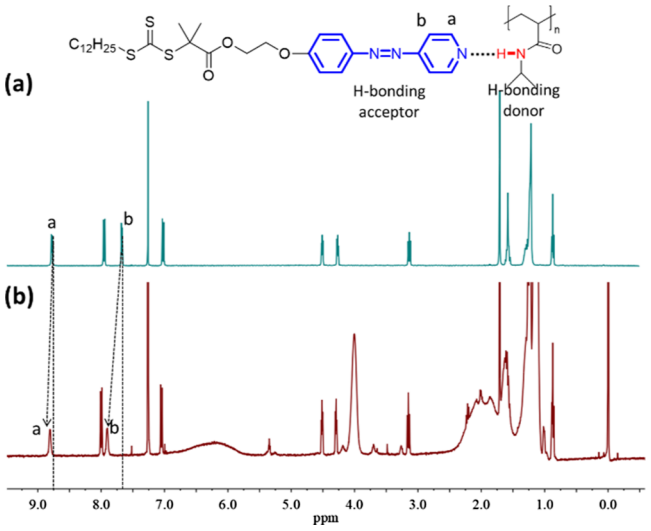

Figure 5. ^{1}H NMR spectra of (a) CTA-AzPy and (b) a supermolecular complex of PNIPAM and CTA-AzPy with solvent $CDCl_3$.

We measured the FTIR spectrum of an intimate solid mixture of PNIPAM and CTA to gain further evidence of the occurrence of H-bonds between the CTA and the PNIPAM amides. The bands ascribed to N−H vibrations in the FTIR spectrum of the mixture (Figure 6) were fitted to the sum of three bands: a band at 3455 cm^{-1} attributed to the stretching vibration of free N−H bonds, a band around 3286 cm^{-1}, indicative of the presence of hydrogen-bonded N−H bonds, and a band at 3294 cm^{-1}. The bands at 3455 and ∼3300 cm^{-1} are also observed in the spectrum of PNIPAM. We attribute the additional band at 3294 cm^{-1} to the stretching vibration of N−H hydrogen-bonded to the azopyridine nitrogen (Figure 6b).[42−44]

The morphology of a C12-PN-AzPy 7K micelle in neutral aqueous solutions (Scheme 2, middle) consists of an *n*-dodecyl core surrounded by AzPy groups confined in a restricted environment through H-bonds to PNIPAM chains, possibly close to the core in view of their hydrophobicity and the limited hydration of the PNIPAM chains confined close to the core.[39,45,46]

The UV−vis absorption spectrum of C12-PN-AzPy 7K in a pH 10 aqueous environment undergoes significant changes upon irradiation of the sample: the band at 350 nm attributed to the $\pi-\pi^*$ transition decreases rapidly, whereas the band at

DOI: 10.1021/acs.macromol.9b00193
Macromolecules 2019, 52, 2939−2948

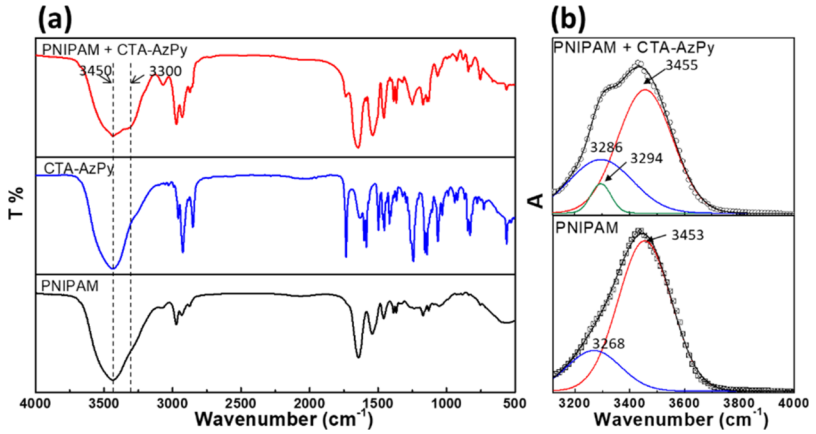

Figure 6. (a) FTIR spectra of PNIPAM (bottom black curve); CTA-AzPy (middle, blue trace) and a mixture of PNIPAM and CTA-AzPy (top, red trace); (b) fitting of the N−H stretching frequency region of the FTIR spectra of PNIPAM homopolymer and the PNIPAM/CTA mixture.

430 nm attributed to n−π* transition grows in. The thermal cis-to-trans isomerization takes over 2 h (Figure 4b, pH = 10), which is typical of neutral azopyridine in which the nitrogen electronic doublet is retained. Indeed, the electron-rich azopyridine nitrogen is unlikely to form hydrogen bonds with hydroxyl anions known to be a strong H-bond acceptor[47,48] and can interact with the amide hydrogen of the PNIPAM repeat unit. We measured the cis-to-trans thermal relaxation time of C12-PN-Azo nanoparticles in water of pH 10. This polymer is a good model of C12-PN-AzPy in terms of self-assembly characteristics, but the azobenzene end group is unable to form H-bonds. Its relaxation time in water is similar to that of C12-PN-AzPy in an alkaline environment (Figure S16).

These photophysical properties, together with the LS results described above, lead us to conclude that C12-PN-AzPy micelles in an pH 10 medium also adopt a core−shell morphology. The precise morphology of the micelles cannot be ascertained from the data obtained so far. Further characterization by SANS or SAXS is needed to determine if the AzPy groups cluster within the micelle core or clustered in the vicinity of the core, as shown in Scheme 2 (right).

4. CONCLUSIONS

When an amphiphilic copolymer is placed in contact with water, the hydrophobic moieties try to minimize contact with water and self-assemble. The segregation of the hydrophobic and hydrophilic components can be mitigated by attractive interactions between the two components through dipole−dipole interactions or hydrogen bonds. The balance of the opposite effects determines the morphology of the copolymer micelles. Routine physicochemical micelle characterization methods often fail to detect intercomponent complexation. The phenomenon can reveal itself through the emergence of unique macroscopic properties, as reported recently in a study of poly-lactide-*b*-poly(-2-isopropyl-2-oxazoline) micelles in water.[49] In the course of this study of azopyridine-end-modified PNIPAM dispersed in neutral aqueous media, we recorded an exceptionally fast cis-to-trans thermal relaxation of the chromophore attributed to the formation of H-bonds between AzPy and PNIPAM chains. The "flower micelle" morphology typical of α,ω-hydrophobically modified PNIPAMs cannot account for this observation. We postulate a micelle morphology consisting of a core of segregated hydrophobes linked to one chain end. The other types of hydrophobes are distributed throughout the micelle PNIPAM shell. Their location within the shell depends on the pH of the aqueous environment. This unique morphology is responsible for the fast photoresponse of the chromophore and its sensitivity to the environment pH.

■ ASSOCIATED CONTENT

Supporting Information

The Supporting Information is available free of charge on the ACS Publications website at DOI: 10.1021/acs.macromol.9b00193.

Synthesis and characterization of RAFT agents and end functional PNIPAMs as well as the characterization of the self-assembly structure, hydrolysis tests, and UV-responsive properties of end-functionalized PNIPAMs (PDF)

■ AUTHOR INFORMATION

Corresponding Author

*E-mail: francoise.winnik@helsinki.fi.

ORCID

Peng Yang: 0000-0002-0463-1024

Françoise M. Winnik: 0000-0001-5844-6687

Notes

The authors declare no competing financial interest.

■ ACKNOWLEDGMENTS

This work was supported in part by the scholarship from China Scholarship Council (CSC) under the Grant CSC no.201606880016 to HR. FMW acknowledges the Natural Sciences and Engineering Research Council of Canada for partial support of this work. We thank Prof. Haifeng Yu (Peking University) and Dr. Xuewei Zhang (University of Montreal) for helpful discussion, Drs. P. M. Aguiar and C. Malveau (University of Montreal) for their help in running NMR diffusion experiments, and Dr. F. Tao (Shaanxi Normal University) for his help for the TEM imaging. HR especially wishes to thank his family for their support over the years.

■ REFERENCES

(1) Jochum, F. D.; Theato, P. Temperature- and light-responsive smart polymer materials. *Chem. Soc. Rev.* **2013**, *42*, 7468−7483.

DOI: 10.1021/acs.macromol.9b00193
Macromolecules 2019, 52, 2939−2948

(2) Trenor, S. R.; Shultz, A. R.; Love, B. J.; Long, T. E. Coumarins in Polymers: From Light Harvesting to Photo-Cross-Linkable Tissue Scaffolds. *Chem. Rev.* **2004**, *104*, 3059−3078.
(3) Zhao, Y. Light-Responsive Block Copolymer Micelles. *Macromolecules* **2012**, *45*, 3647−3657.
(4) Bandara, H. M. D.; Burdette, S. C. Photoisomerization in different classes of azobenzene. *Chem. Soc. Rev.* **2012**, *41*, 1809−1825.
(5) Ren, H.; Chen, D.; Shi, Y.; Yu, H.; Fu, Z.; Yang, W. Charged End-Group Terminated Poly(N-isopropylacrylamide)-b-poly-(carboxylic azo) with Unusual Thermoresponsive Behaviors. *Macromolecules* **2018**, *51*, 3290−3298.
(6) Garcia-Amorós, J.; Massad, W. A.; Nonell, S.; Velasco, D. Fast Isomerizing Methyl Iodide Azopyridinium Salts for Molecular Switches. *Org. Lett.* **2010**, *12*, 3514−3517.
(7) Bujak, K.; Orlikowska, H.; Małecki, J. G.; Schab-Balcerzak, E.; Bartkiewicz, S.; Bogucki, J.; Sobolewska, A.; Konieczkowska, J. Fast dark cis-trans isomerization of azopyridine derivatives in comparison to their azobenzene analogues: Experimental and computational study. *Dyes Pigments* **2019**, *160*, 654−662.
(8) Ruokolainen, J.; Makinen, R.; Torkkeli, M.; Makela, T.; Serimaa, R.; Brinke, G.; Ikkala, O. Switching supramolecular polymeric materials with multiple length scales. *Science* **1998**, *280*, 557−560.
(9) Millaruelo, M.; Chinelatto, L. S.; Oriol, L.; Piñol, M.; Serrano, J.-L.; Tejedor, R. M. Synthesis and Characterization of Supramolecular Polymeric Materials Containing Azopyridine Units. *Macromol. Chem. Phys.* **2006**, *207*, 2112−2120.
(10) Mallia, V. A.; Antharjanam, P. K. S.; Das, S. Synthesis and studies of some 4-substituted phenyl-4′-azopyridine-containing hydrogen-bonded supramolecular mesogens. *Liq. Cryst.* **2003**, *30*, 135−141.
(11) Cui, L.; Zhao, Y. Azopyridine Side Chain Polymers: An Efficient Way To Prepare Photoactive Liquid Crystalline Materials through Self-Assembly. *Chem. Mater.* **2004**, *16*, 2076−2082.
(12) Sun, S.-S.; Lees, A. J.; Zavalij, P. Y. Highly Sensitive Luminescent Metal-Complex Receptors for Anions through Charge-Assisted Amide Hydrogen Bonding. *Inorg. Chem.* **2003**, *42*, 3445−3453.
(13) Liu, X.-M.; Xie, L.-H.; Lin, J.-B.; Lin, R.-B.; Zhang, J.-P.; Chen, X.-M. Flexible porous coordination polymers constructed from 1,2-bis(4-pyridyl)hydrazine via solvothermal in situ reduction of 4,4′-azopyridine. *Dalton Trans.* **2011**, *40*, 8549−8554.
(14) Aoki, K.; Nakagawa, M.; Ichimura, K. Self-Assembly of Amphoteric Azopyridine Carboxylic Acids: Organized Structures and Macroscopic Organized Morphology Influenced by Heat, pH Change, and Light. *J. Am. Chem. Soc.* **2000**, *122*, 10997−11004.
(15) Zhang, H.; Hao, R.; Jackson, J. K.; Chiao, M.; Yu, H. Janus ultrathin film from multi-level self-assembly at air-water interfaces. *Chem. Commun.* **2014**, *50*, 14843−14846.
(16) Gelebart, A. H.; Jan Mulder, D.; Varga, M.; Konya, A.; Vantomme, G.; Meijer, E. W.; Selinger, R. L. B.; Broer, D. J. Making waves in a photoactive polymer film. *Nature* **2017**, *546*, 632−636.
(17) Shen, G.; Xue, G.; Cai, J.; Zou, G.; Li, Y.; Zhang, Q. Photo-induced reversible uniform to Janus shape change of vesicles composed of PNIPAM-b-PAzPy2. *Soft Matter* **2013**, *9*, 2512−2517.
(18) Xue, G.; Chen, K.; Shen, G.; Wang, Z.; Zhang, Q.; Cai, J.; Li, Y. Phase-separation and photoresponse in binary azobenzene-containing polymer vesicles. *Colloids Surf., A* **2013**, *436*, 1007−1012.
(19) Han, K.; Su, W.; Zhong, M.; Yan, Q.; Luo, Y.; Zhang, Q.; Li, Y. Reversible Photocontrolled Swelling-Shrinking Behavior of Micron Vesicles Self-Assembled from Azopyridine-Containing Diblock Copolymer. *Macromol. Rapid Commun.* **2008**, *29*, 1866−1870.
(20) Lin, W.-C.; Tsai, M.-C.; Rajappa, R.; Kramer, R. H. Design of a Highly Bistable Photoswitchable Tethered Ligand for Rapid and Sustained Manipulation of Neurotransmission. *J. Am. Chem. Soc.* **2018**, *140*, 7445−7448.
(21) Jerca, V. V.; Jerca, F. A.; Rau, I.; Manea, A. M.; Vuluga, D. M.; Kajzar, F. Advances in understanding the photoresponsive behavior of azobenzenes substituted with strong electron withdrawing groups. *Opt. Mater.* **2015**, *48*, 160−164.
(22) Wei, J.; Yan, Z.; Lin, L.; Gu, J.; Feng, Z.; Yu, Y. Photo/pH dual-responsive behavior of azopyridine-containing copolymer vesicles. *React. Funct. Polym.* **2013**, *73*, 1009−1014.
(23) Liu, G.-F.; Ji, W.; Feng, C.-L. Installing Logic Gates to Multiresponsive Supramolecular Hydrogel Co-assembled from Phenylalanine Amphiphile and Bis(pyridinyl) Derivative. *Langmuir* **2015**, *31*, 7122−7128.
(24) Keddie, D. J.; Moad, G.; Rizzardo, E.; Thang, S. H. RAFT Agent Design and Synthesis. *Macromolecules* **2012**, *45*, 5321−5342.
(25) Chen, Y.; Yu, H.; Zhang, L.; Yang, H.; Lu, Y. Photoresponsive liquid crystals based on halogen bonding of azopyridines. *Chem. Commun.* **2014**, *50*, 9647−9649.
(26) Wang, X.; Wu, C. Light-Scattering Study of Coil-to-Globule Transition of a Poly(N-isopropylacrylamide) Chain in Deuterated Water. *Macromolecules* **1999**, *32*, 4299−4301.
(27) Chen, Y.; Quan, M.; Yu, H.; Zhang, L.; Yang, H.; Lu, Y. Fabrication of nanofibres with azopyridine compounds in various acids and solvents. *RSC Adv.* **2015**, *5*, 31219−31225.
(28) Koga, T.; Tanaka, F.; Motokawa, R.; Koizumi, S.; Winnik, F. M. Theoretical Modeling of Associated Structures in Aqueous Solutions of Hydrophobically Modified Telechelic PNIPAM Based on a Neutron Scattering Study. *Macromolecules* **2008**, *41*, 9413−9422.
(29) Kujawa, P.; Segui, F.; Shaban, S.; Diab, C.; Okada, Y.; Tanaka, F.; Winnik, F. M. Impact of End-Group Association and Main-Chain Hydration on the Thermosensitive Properties of Hydrophobically Modified Telechelic Poly(N-isopropylacrylamides) in Water. *Macromolecules* **2006**, *39*, 341−348.
(30) Kujawa, P.; Tanaka, F.; Winnik, F. M. Temperature-Dependent Properties of Telechelic Hydrophobically Modified Poly(N-isopropylacrylamides) in Water: Evidence from Light Scattering and Fluorescence Spectroscopy for the Formation of Stable Mesoglobules at Elevated Temperatures. *Macromolecules* **2006**, *39*, 3048−3055.
(31) Kokufuta, E.; Ogawa, K.; Doi, R.; Kikuchi, R.; Farinato, R. S. Geometrical Characteristics of Polyelectrolyte Nanogel Particles and Their Polyelectrolyte Complexes Studied by Dynamic and Static Light Scattering†. *J. Phys. Chem. B* **2007**, *111*, 8634−8640.
(32) Yang, F.; Cao, Z.; Wang, G. Micellar assembly of a photo- and temperature-responsive amphiphilic block copolymer for controlled release. *Polym. Chem.* **2015**, *6*, 7995−8002.
(33) Yao, C.; Wang, X.; Liu, G.; Hu, J.; Liu, S. Distinct Morphological Transitions of Photoreactive and Thermoresponsive Vesicles for Controlled Release and Nanoreactors. *Macromolecules* **2016**, *49*, 8282−8295.
(34) Greenspan, P.; Mayer, E. P.; Fowler, S. D. Nile red: a selective fluorescent stain for intracellular lipid droplets. *J. Cell Biol.* **1985**, *100*, 965−973.
(35) Greenspan, P.; Fowler, S. D. Spectrofluorometric studies of the lipid probe, nile red. *J. Lipid Res.* **1985**, *26*, 781−789.
(36) Buncel, E.; Keum, S.-R. Studies of azo and azoxy dyestuffs-16 Investigations of the protonation and tautomeric equilibria of 4-(p'-hydroxyphenylazo)pyridine and related substrates. *Tetrahedron* **1983**, *39*, 1091−1101.
(37) Willcock, H.; O'Reilly, R. K. End group removal and modification of RAFT polymers. *Polym. Chem.* **2010**, *1*, 149−157.
(38) Skrabania, K.; Miasnikova, A.; Bivigou-Koumba, A. M.; Zehm, D.; Laschewsky, A. Examining the UV-vis absorption of RAFT chain transfer agents and their use for polymer analysis. *Polym. Chem.* **2011**, *2*, 2074−2083.
(39) Garcia-Amorós, J.; Velasco, D. Recent advances towards azobenzene-based light-driven real-time information-transmitting materials. *Beilstein J. Org. Chem.* **2012**, *8*, 1003−1017.
(40) Yu, H.; Liu, H.; Kobayashi, T. Fabrication and Photoresponse of Supramolecular Liquid−Crystalline Microparticles. *ACS Appl. Mater. Interfaces* **2011**, *3*, 1333−1340.
(41) Bryant, R. G. The NMR time scale. *J. Chem. Educ.* **1983**, *60*, 933−935.
(42) Coleman, M. M.; Skrovanek, D. J.; Hu, J.; Painter, P. C. Hydrogen bonding in polymer blends. 1. FTIR studies of urethane-ether blends. *Macromolecules* **1988**, *21*, 59−65.

DOI: 10.1021/acs.macromol.9b00193
Macromolecules 2019, 52, 2939−2948

(43) Laurence, C.; Brameld, K. A.; Graton, J.; Le Questel, J.-Y.; Renault, E. The pKBHXDatabase: Toward a Better Understanding of Hydrogen-Bond Basicity for Medicinal Chemists. *J. Med. Chem.* **2009**, *52*, 4073−4086.
(44) Yamada, T.; Ichino, T.; Hanyu, M.; Ninomiya, D.; Yanagihara, R.; Miyazawa, T.; Murashima, T. A novel intramolecular hydrogen bonding between a side-chain pyridine ring and an amide hydrogen of the peptide backbone in tripeptides containing the new amino acid, α,α-di(2-pyridyl)glycine. *Org. Biomol. Chem.* **2004**, *2*, 2335−2339.
(45) Gavezzotti, A.; Filippini, G. Geometry of the Intermolecular X-H···Y (X, Y = N, O) Hydrogen Bond and the Calibration of Empirical Hydrogen-Bond Potentials. *J. Phys. Chem.* **1994**, *98*, 4831−4837.
(46) Pimentel, G. C.; Sederholm, C. H. Correlation of Infrared Stretching Frequencies and Hydrogen Bond Distances in Crystals. *J. Chem. Phys.* **1956**, *24*, 639−641.
(47) Abu-Dari, K.; Raymond, K. N.; Freyberg, D. P. The bihydroxide (H3O2-) anion. A very short, symmetric hydrogen bond. *J. Am. Chem. Soc.* **1979**, *101*, 3688−3689.
(48) Tuckerman, M. E.; Marx, D.; Parrinello, M. The nature and transport mechanism of hydrated hydroxide ions in aqueous solution. *Nature* **2002**, *417*, 925−929.
(49) Pooch, F.; Sliepen, M.; Knusden, K. D.; Nystrom, B.; Tenhu, H.; Winnik, F. M. Poly(2-isopropyl-2-oxazoline)-b-Poly(lactide) (PiPOx-b-PLA) nanoparticles in water: interblock van der Waals attraction opposes amphiphilic phase separation. *Macromolecules* **2019**, *52*, 1317−1326.

DOI: 10.1021/acs.macromol.9b00193
Macromolecules 2019, 52, 2939−2948